EPR and optical properties of $KY(WO_4)_2$:Gd^{3+} powders

Grzegorz Leniec[a)]
West Pomeranian University of Technology, Faculty of Mechanical Engineering and Mechatronics, Institute of Physics, 70-310 Szczecin, Poland

Lucyna Macalik
Institute of Low Temperature and Structure Research, PAS, 50-950 Wrocław, Poland

Sławomir Maksymilian Kaczmarek and Tomasz Skibiński
West Pomeranian University of Technology, Faculty of Mechanical Engineering and Mechatronics, Institute of Physics, 70-310 Szczecin, Poland

Jerzy Hanuza
Institute of Low Temperature and Structure Research, PAS, 50-950 Wrocław, Poland

(Received 28 March 2012; accepted 6 September 2012)

Comparisons of structural, optical, and magnetic properties between $KY(WO_4)_2$ (KYW) powders doped with Gd^{3+} from 0.5 up to 100 mol% and $KGd(WO_4)_2$ and KYW single crystals have been made. For this purpose, x-ray diffraction (XRD), infrared (IR), Raman, and electron paramagnetic resonance (EPR) spectra were collected. The XRD studies have verified the quality of the synthesis of compounds and have shown the differences in the positions of the diffraction peaks due to the change in concentration of gadolinium ions. Raman and IR spectra confirmed that the phases are isostructural. The optimization of the spin Hamiltonian parameters and EPR data simulation was achieved by using the electron paramagnetic resonance and nuclear magnetic resonance (EPR-NMR) program. Changes in kind of magnetic interactions were found and analyzed from the point of view of their dependence of the compound form (powder, single crystal), temperature, and gadolinium ion concentration. The investigated compounds revealed complex interactions between gadolinium ions both in a type and a strength.

I. INTRODUCTION

Double tungstates containing rare-earth ions are attractive laser host materials due to very high stability of emission, high efficiency, long lifetime, and low excitation threshold as well as excellent chemical and thermal durability in air. This group of crystals is good candidate for efficient stimulated Raman scattering as well as for fabrication of high efficiency lasers with high output energy.[1] They create a family of compounds with general formula $A^{I}RE^{III}(W^{VI}O_4)_2$ where A denotes an alkali metal ion and RE denotes a rare-earth ion. These compounds crystallize in the structure, whose prototype is the scheelite- or wolframite-type structure. RE^{3+} and A^{+} ions can be coordinated by oxygen ions and have 8 and 12 coordinated number, respectively. Rare-earth oxygen polyhedra form square antiprism units, while the alkali metal polyhedra form distorted icosahedron units. In dependence of kind of alkali metal, tungsten atoms build isolated WO_4 tetrahedra or deformed WO_6 octahedra connected by a common edge forming double chains of W_2O_{10}.[2–6]

The $KY(WO_4)_2$ (KYW) and $KGd(WO_4)_2$ (KGW) tungstates crystallize in the monoclinic structure C2/c = C_{2h}^6 with $Z = 4$.[4,7] In this structure, the tungstate units built the WO_6 octahedra joined through the single and double oxygen bridges. The RE^{3+} ions occupy the sites of C_1 and C_2 symmetry. These materials reveal polymeric structure. Raman spectra show the bands in the gap region between 450 and 750 cm^{-1} where the stretching modes of the $M^{O}M$ and $M_{O}{}^{O}M$ oxygen bonds are observed.[2] Spectroscopic *g* factor shows anomaly at low temperatures suggesting the presence of some kind of internal magnetic fields, assigned, e.g., to one-dimensional (1D) chains.[8]

Due to the structure, we have chosen electron paramagnetic resonance (EPR) technique, besides Raman spectra analysis, to find clear differences between KGW single crystal and KGW powder samples.

Magnetic properties of KGW single crystals were analyzed in detail by Borowiec et al.,[9] but our findings differ from them due to wider range of investigated temperatures taken into account in our measurements. For comparison, we have taken single crystals of the above stoichiometry: KYW and KGW and powder samples of KYW tungstate variously doped with gadolinium. Diluted and concentrated materials should differ for many features. The aim of this paper was to find differences in structure, kind of magnetic interactions, and local symmetry of the compounds having various form and different concentration of gadolinium ions.

[a)]Address all correspondence to this author.
e-mail: gleniec@zut.edu.pl
DOI: 10.1557/jmr.2012.345

II. EXPERIMENTAL

Starting materials: KNO_3 (99.9%, Sigma-Aldrich Co., St. Louis, MO), rare-earth Y_2O_3 and Gd_2O_3 oxides (99.9%, Aldrich), and WO_3 (99.9%, Fluka Chemie AG, Buchs, Switzerland) were used for powder synthesis. Before use, the rare-earth oxides were heated in air at 1123 K for 12 h to remove adsorbed traces of water and carbon dioxide. First, the polycrystalline sample of potassium tungstate was obtained. For this purpose, the KNO_3/WO_3 mixture was heated in air at 893 K for 12 h. After cooling to room temperature, the sample was reground and heated again three times at 1013 K for 12 h to complete the reaction according to the equation:

$$4KNO_{3(s)} + 2WO_{3(s)} = 2K_2WO_{4(s)} + 4NO_{2(g)} + O_{2(g)} \quad . \tag{1}$$

The final product was checked by x-ray diffraction (XRD) method and characterized as the monoclinic potassium tungstate, K_2WO_4, with C2/m symmetry.[10] The polycrystalline samples of KGW and the $KY_{1-x}Gd_x(WO_4)_2$ solid solutions ($x = 0.005$, 0.10, and 0.20) were prepared by the solid-state reaction according to the Eqs. (2) and (3), respectively.

$$K_2WO_{4(s)} + Gd_2O_{3(s)} + 3WO_{3(s)} = 2KGd(WO_4)_{2(s)} \quad , \tag{2}$$

$$K_2WO_{4(s)} + (1-x)Y_2O_{3(s)} + xGd_2O_{3(s)} + 3WO_{3(s)} = 2KY_{1-x}Gd_x(WO_4)_{2(s)} \quad . \tag{3}$$

Stoichiometric amounts of K_2WO_4, Gd_2O_3, and WO_3 as well as K_2WO_4, Y_2O_3, Gd_2O_3, and WO_3 were mixed homogeneously in an agate mortar. Next, they were sintered in corundum crucible several times, during 12-h periods, at selected temperatures from 873 to 1083 K. After each heating period, all samples were cooled to ambient temperature and ground. The powder diffraction patterns of prepared samples were in good agreement with the literature data for KGW and KYW.[11] The indication of gadolinium content is nominal but the doping in this kind of material is proceeded easily as it is resulted from our previous experience; the $KY_{1-x}Gd_x(WO_4)_2$ compounds are stoichiometric.

KYW and KGW single crystals were grown by a low gradient Czochralski technique (modified top-seeded solution method) in Pt crucibles using oriented seeds along the crystallographic *b*-axis. All the samples were checked for purity by the x-ray powder diffraction, infrared (IR) absorption spectra, Raman, and EPR spectra.

XRD powder patterns of the powder samples were recorded at room temperature by using X'Pert PRO powder diffractometer (PANalytical, Almelo, Netherlands) working in the reflection geometry and using Cu $K_{\alpha 1}$ radiation in the 2θ range from 10° to 65° with a step of 0.026°.

The IR absorption spectra were measured with a BioRad 575C FTIR spectrometer (Bio-Rad Laboratories Inc., Benicia, CA) in KBr pellets for the 1000–400 cm^{-1} region and in Nujol suspension for the 500–50 cm^{-1} region. Raman spectra were measured using a Bruker RFS 100/S Raman spectrometer (Bruker Optic GmbH, Ettlingen, Germany) with the backscattering configuration. The 1064-nm line of Nd:YAG laser was used as an excitation. Signal detection was performed with the LN–Ge (D418-T) liquid nitrogen-cooled NIR detector (Bruker Optik GmbH, Ettlingen, Germany) with an integrated preamplifier and high voltage power supply. The resolution of the Raman and IR measurements was 2 cm^{-1}.

EPR spectra were recorded on a conventional X-band Bruker ELEXSYS E 500 CW-spectrometer (Bruker Analytik GmbH, Rheinstetten, Germany) operating at 9.5 GHz with a 100-kHz magnetic field modulation. The investigated samples were in fine powder form [besides, KGW and KYW single crystals]. The first derivative of the powder absorption spectra has been recorded as a function of the applied magnetic field. Temperature dependence of the EPR spectra of the powder samples in the 80–300 K temperature range was recorded using an Oxford Instruments ESP nitrogen-flow cryostat (Oxford Instruments Ltd., Witney, UK). EPR-NMR program was applied to recognize spin Hamiltonian parameters for comparison purpose.[12]

III. RESULTS AND DISCUSSION

A. XRD measurements

The purity and structure of $KY_{1-x}Gd_x(WO_4)_2$ powders (signed later as KYW:Gd) were checked by the x-ray powder diffraction. Figure 1 shows the XRD profiles of measured samples together with the characteristic reflections of KYW (ICSD Collection Code No. 90378) and KGW

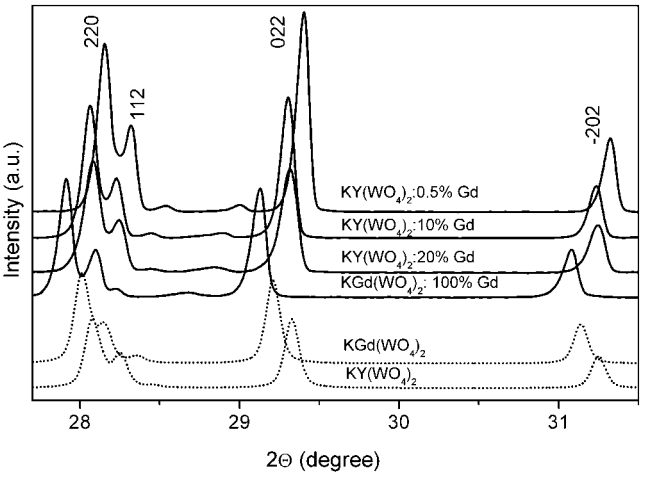

FIG. 1. X-ray powder diffraction patterns of the double potassium lanthanide tungstates with the patterns of corresponding crystals for comparison (KYW—ICSD No. 90378, KGW—ICSD No. 68249).

(ICSD Collection Code No. 68249) single crystal enlarged from 27.7° to 31.5° to show the distinct differences. Line assignment has been done according to the International Center for Diffraction Data (PDF Card No. 01-080-0455) using the published structural data.[5,13,14] The XRD results for pure and Gd-doped KYW samples confirm that they crystallize in the monoclinic system with the C2/c space group. The recorded x-ray patterns presented in Fig. 1 are almost identical for all phases in respect of number of peaks and their mutual intensity. The slight displacement of lines for powder samples and crystals are due to differences in zero correction for both experiments made with different diffractometers. The crystalline nature and lattice parameters of KYW:Gd do not change much from the values for pure KYW. Increase of the gadolinium ions concentration does not also influence the crystalline structure; the Gd^{3+} ions occupy the same positions as Y^{3+}.[5] KYW and KGW crystallographic structure was described in detail in previous works.[2,7,15]

Nevertheless, there are some differences in positions of diffraction peaks between the patterns. Peaks of KYW are shifted slightly toward high angle side if compared to those of KGW. Situation is the same for the powders; the shift toward the higher angles is the biggest for KYW:0.5% mol Gd^{3+}. This tendency is expected and reflects the differences in lattice constants. Ionic radius of Gd^{3+} and Y^{3+} equals to 1.060 and 1.015 Å, respectively[16]; the lattice parameters for KYW are less and their diffraction patterns are represented at the higher angles. The lattice parameters for $KY_{1-x}Gd_x(WO_4)_2$ powder samples calculated from the XRD data using powder diffraction data analysis software are shown in Table I. These parameters have been taken from the indexing of the powder diagram for equivalent crystallographic description to I2/c space group. The dependence of unit cell parameters on values of gadolinium concentration is almost linear that confirms the assumed gadolinium concentration.

B. IR and Raman spectra

Figures 2(a) and 2(b) show the IR spectra in the far- and midrange for gadolinium ions variously doped KYW powders. The IR spectra of all phases consist of group of bands in the 720–1000 cm^{-1} range, two strong and broad bands in the 550–680 cm^{-1} range, two bands of medium intensity in the 420–500 cm^{-1} range, and several medium intensity bands in the 260–420 cm^{-1} range [Fig. 2(a)]. They reflect stretching and bending vibrations of W–O and oxygen bridge bonds.[7,15] Some distinct differences can be observed in peak positions of the absorption bands between the phases. Peaks of KGW absorption bands are clearly shifted toward lower wave number when compare to KYW and gadolinium ions-doped KYW. The bands below 260 cm^{-1} differ noticeably for bulk KGW in compare to the others. They reflect the external vibrations:

TABLE I. Lattice parameters for monoclinic $KY_{1-x}Gd_x(WO_4)_2$, for I2/c space group.

x	a (Å)	b (Å)	c (Å)	β (degree)	V (Å^3)
0.005	8.0745	10.3382	7.5541	94.340	628.78
0.1	8.0765	10.3449	7.5570	94.334	629.59
0.2	8.0803	10.3530	7.5671	94.263	631.28
1	8.1152	10.4383	7.6018	94.394	642.05

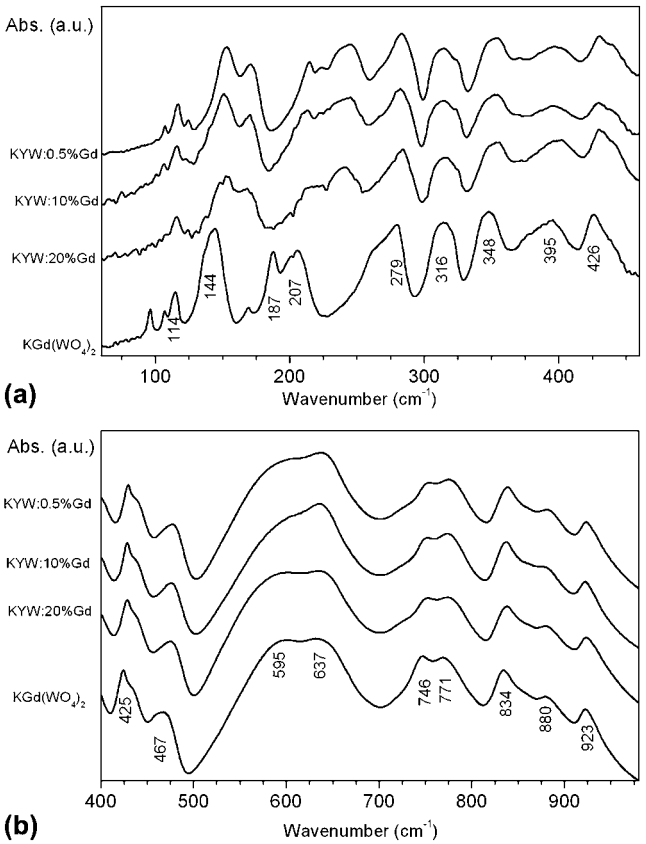

FIG. 2. IR spectra in the (a) far- and (b) midrange of the Gd^{3+}-doped KYW powders.

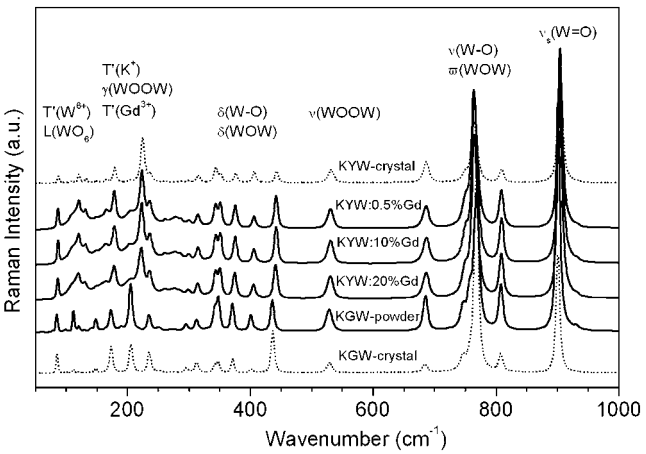

FIG. 3. Raman spectra of the Gd^{3+}-doped KYW powders and single crystals.

translatory and libratory lattice modes, which are coupled with the low-energy vibrations of the oxygen bridges. Translatory modes of the gadolinium ions T′(Gd^{3+}) are observed at 206 and 188 cm^{-1} and modes of the yttrium ions T′(Y^{3+}) at about 223 cm^{-1}.[7,15]

In Fig. 3, Raman spectra of the analyzed samples are presented. Raman spectra of doped gadolinium ions double tungstates are almost identical for the three concentrations of Gd^{3+} ions. They consist of multiplets of the stretching W–O vibrations showing four strong bands in the 740–1000 cm^{-1} range and the bending vibrations with medium intensity bands in the 270–470 cm^{-1} range. The appearance of the medium intensity bands in the range of 500–700 cm^{-1} of Raman spectra is confirmation of the KYW and KGW polymeric structure. In this region, the stretching modes of oxygen bridge bonds are observed. They play an important role in the electron–phonon coupling and consequently in the energy transfer in these crystals. The group of medium bands in the 70–260 cm^{-1} range corresponds to the external modes connected with the translational motions and vibrations of the tungstate polyhedra. The assignment to the respective normal modes presented in Fig. 3 was done according to the previous works.[2,7,15] The spectra for both powdered and KGW single crystal are the same as for the doped tungstates regarding the number of bands with simultaneous shift of a large majority of bands toward lower wave numbers. In the present studies, T′(K^{+}) modes are observed at 236 cm^{-1} and translatory modes of the lanthanide ions T′(Gd^{3+}) and T′(Y^{3+}) are observed at about 205 and 222 cm^{-1}, respectively.

C. EPR spectra of KYW:Gd^{3+} powders

The electron configuration of Gd^{3+} is [Xe]$4f^7$; hence, the spin quantum number, S, is 7/2 and the ground state of Gd^{3+} is $^8S_{7/2}$. The state $^8S_{7/2}$ splits into $2S + 1 = 8$ states; then, the seven allowed transitions according to the selection rule, $\Delta M_S = \pm 1$, are obtained.

As could be seen from Figs. 4 and 5, some of the lines of fine structure could be clearly seen. Usually, between the lines, hyperfine structure lines could be also observed, arising from isotopes $^{157}Gd^{3+}$ ($I = 3/2$) and $^{155}Gd^{3+}$ ($I = 3/2$),[17] but in our samples, we could not recognize the lines. The EPR signal with a fine structure originates from the isolated gadolinium ions. It has been known that crystal fields of the KGW interact weakly with the $^8S_{7/2}$ ground state of Gd^{3+}. The crystal field splitting for Gd^{3+} is generally smaller than that produced by the Zeeman interaction in the x-band electron spin resonance (ESR) experiments. So, the EPR spectra can be described by a spin Hamiltonian incorporating with Zeeman interaction and crystal field operators (neglecting hyperfine interactions) in the form of the following equation[18]:

$$H = H_{\mathrm{ZEEMAN}} + H_{\mathrm{exch}} + H_{\mathrm{SS}} \quad ,$$

$$H = g_0 \mu_B B S + J S_1 S_2 + D[S_z^2 - (1/3)S(S+1)] + E(S_x^2 - S_y^2) \quad , \qquad (4)$$

where H_{ZEEMAN} term with B—magnetic field, μ_B is Bohr magneton, and S_x, S_y, S_z are electron spin operators, H_{exch} is a Hamiltonian of electron exchange interaction with an isotropic electron exchange coupling constant, J, H_{SS} is a Hamiltonian of dipolar electron spin interaction with D and E being the zero field splitting constants (reflects the local symmetry of the crystal); the value of g—factor of the ion—is isotropic and equals to g_0 as in a case of free ion.

Room temperature EPR spectra for the investigated KYW powders doped with 0.5, 10, 20, and 100 mol% of Gd^{3+} ions and comparative KGW single crystal are presented in Fig. 4. The resolution of the lines is better for lower concentrations of gadolinium. For the fourth curve (100 mol% of Gd^{3+}), the EPR signal, as in a case of KGW single crystal, is an envelope of unresolved anisotropic fine

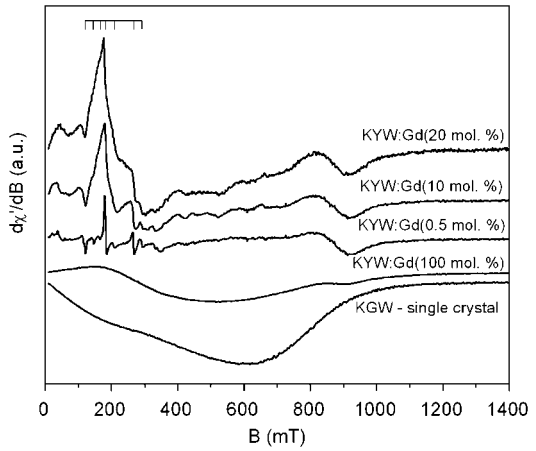

FIG. 4. Room temperature EPR spectra of powdered KYW:Gd^{3+} (0.5, 10, 20, and 100 mol%) and KGW single crystal.

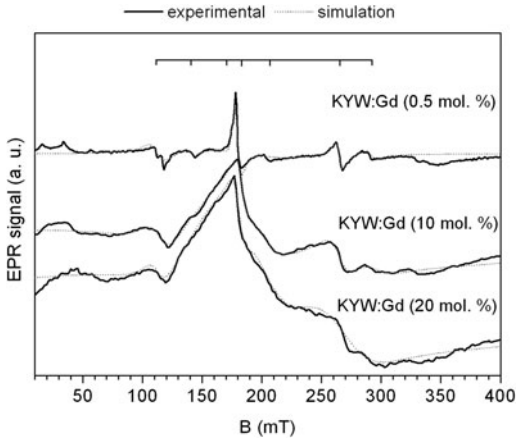

FIG. 5. Experimental room temperature EPR spectra and fitting curves obtained from EPR-NMR program[12] for KYW:Gd^{3+} 0.5, 10, and 20 mol% powders.

TABLE II. Spin Hamiltonian (1) parameters describing EPR spectra of the all investigated powders.

Powder	g_0	$D \times 10^{-4}$ (cm^{-1})	$E \times 10^{-4}$ (cm^{-1})	J (K)
KYW:Gd 0.5 mol%	3.80 (1)	139 (20)	−17 (2)	~0 (10)
KYW:Gd 10 mol%	3.56 (2)	261 (40)	−33 (5)	126 (8)
KYW:Gd 20 mol%	3.57 (2)	284 (40)	−32 (5)	126 (8)
KYW:Gd 100 mol%	1.97 (1)	825 (40)	−275 (10)	250 (15)
KGW	~1.85 (3)	870 (58)	−100 (10)	370 (10)

structure of the Gd^{3+} ions in powder. Applying EPR-NMR program,[12] we were able to find parameters of the spin Hamiltonian (4) for all the investigated powders. The results of the fitting are gathered in Table II.

As one can see from Table II, values of D and E parameters are typical[19] and evolve with a concentration of gadolinium ions according to very well-known rules, e.g., $D \sim 1/R^3$, where R is a distance between Gd^{3+} ions. The results of analysis of other magnetic properties of KGW powders were described in the next part of Sec. III based on the EPR measurements in a range of 80–300 K. In this range of temperature, we expected to observe changes in the type and strength of magnetic interactions.

To find parameters of the resolved spectra, we have applied fitting procedure of the EPR spectra line shapes using superposition of seven Lorentzian functions. Figure 5 shows the effect of the fitting. Solid lines are experimental curves of the EPR spectra; dotted lines are fittings obtained from the above procedure. As could be expected, only in a case of low doping, all fine structure lines are clearly resolved.

Nevertheless, the positions of all resonance lines of the fine structure for all the investigated powders do not depend on the concentration of gadolinium ions. We have found, moreover, that besides seven Lorentzian lines, one wide Gaussian line had to be added to the above superposition to obtain good enough fitting.

The width of the line increases with increase of concentration of Gd^{3+} ions. It indicates the presence of some more complex magnetic entities and their magnetic interactions in the investigated compounds. The conclusion can be verified by performing deconvolution of line shapes of the EPR lines measured at different temperatures. We have performed some fittings for KYW:Gd (10 mol%) solid solution, based on the following equation[20]:

$$\mathrm{OS} = \sum_{i=1}^{7} [C_i L_i + (1 - C_i) G_i] + [F(L_1 + L_2) + (1 - F)(G_1 + G_2)] \quad , \quad (5)$$

where OS is overall shape of the EPR spectrum, L_i and G_i represents Lorentzian and Gaussian shapes of EPR curve, C and F are percentage contributions of a given kind of magnetic interaction to overall interaction (C and $F = 0$—Gaussian shape—dipole–dipole interactions, C and $F = 1$—Lorentzian shape—exchange interactions); the presence of F parameter reflects a wide line share to overall EPR spectrum of gadolinium ions in the compound. Figure 6 shows the dependencies of C and F parameters on a temperature.

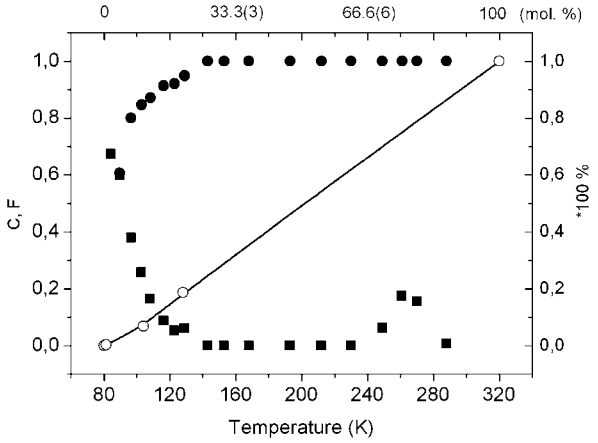

FIG. 6. C (upper curve, circles) and F (bottom curve, squares) parameters of overall shape of the EPR spectrum for KYW:Gd^{3+} 10 mol% (left and bottom scales) and dependence of the share of Gaussian shape in an overall shape of a given EPR spectrum (right and upper scales).

As one can see from Fig. 6 (left and bottom scales), the wide line (F parameter) and a superposition of fine structure (seven lines, C) show mainly Gaussian- or Lorentzian-like line shape above 140 K, respectively. This temperature may be a temperature of structural phase transition or a temperature separating different kinds of magnetic interactions. Because the Raman spectra versus temperature (not added here) had not confirmed conclusion on structural phase transition, the second reason stay actual. So, Gaussian shape of the additional wide line, dominating above 140 K, indicates dipolar interactions between gadolinium ions within local cluster-/chain-like magnetic structure.

We also have performed corresponding fittings of the EPR spectra of the samples under studies and obtained almost linear dependence of the share of Gaussian shape in an overall shape of a given EPR spectrum. For 0.5 mol% of Gd^{3+}, it was 0.3 (9)%; for 10 mol% of Gd^{3+}, it was 6.9 (3)%; for 20 mol% of Gd, it was 18.7 (3)%; and for 100 mol% Gd, it was 100% (see Fig. 6: right and upper scales). It means that the share of dipolar interactions in overall magnetic interactions linearly increases with gadolinium ions content.

As a result of further temperature analysis of the EPR spectra, we have found that the investigated powder samples show basically antiferromagnetic kind of magnetic interactions between gadolinium ions (similarly, as in the case of KGW single crystal). On the other hand, the strength of these interactions is different and depends on the gadolinium concentration and a temperature. The exceptions were found only for compounds with 10 and 20 mol% of Gd^{3+}.

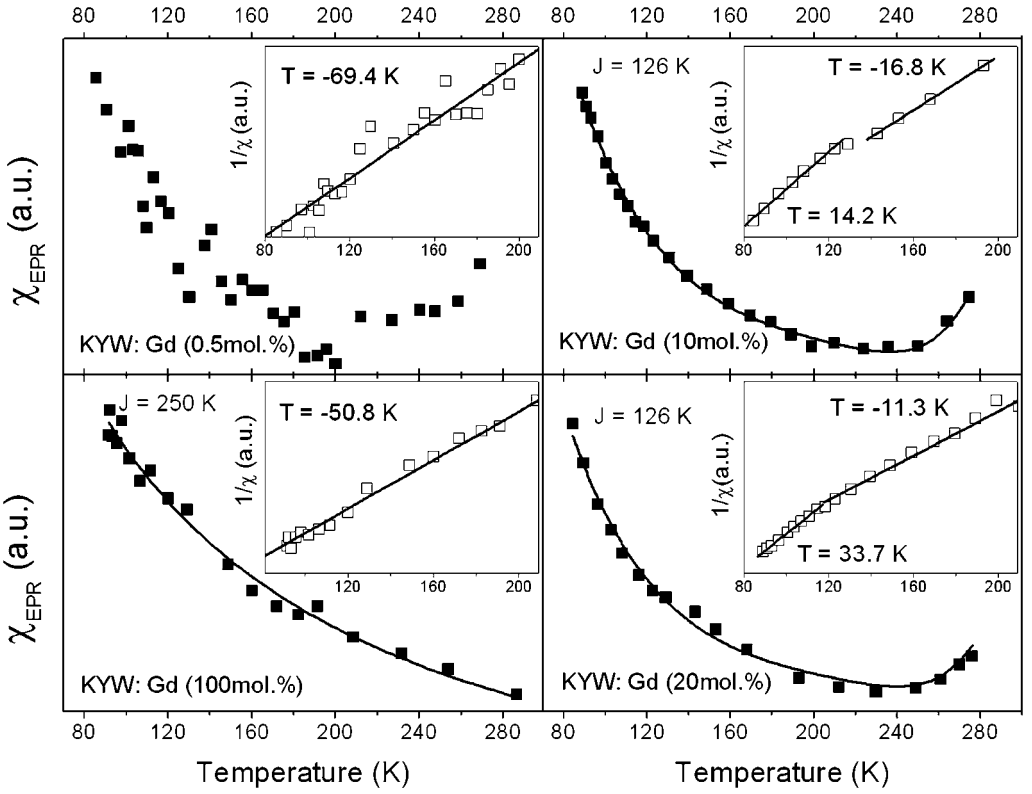

FIG. 7. The integral intensity of the EPR spectra of KYW:Gd^{3+} 0.5, 10, and 20 mol% and KGW compounds. Solid curves reflect the Curie–Weiss law. In the insets, fitting parameters to the law are also collected.

In Fig. 7, we present the overall integral intensity and reciprocal of the integral intensity of EPR spectra of the all phases. Only for one of them, the shape of the integral intensity dependence does not show complex behavior (100 mol%). All others reveal strong deviations from the Curie–Weiss law especially above 240 K. The reason of such behavior may be the following: when gadolinium ions reach a concentration of 10 mol%, clusters of gadolinium ions are expected to be formed, or generally, more complex magnetic entities.[21] Moreover, the investigated phases are polymeric in a structure, so we expect to find some modifications of the shapes of temperature dependences of the EPR spectra, reflecting the presence of, e.g., internal magnetic fields. The evidence of such behavior may supply the analysis of line widths and changes in a position of the resonance lines with the change of a temperature.

The fittings of the curves from Fig. 7 to the Curie–Weiss law allowed finding Curie–Weiss temperatures equal to about −51 K for KGW and −69.4 K for KYW:Gd^{3+} 0.5 mol% powders. It indicates strong antiferromagnetic interactions between gadolinium ions in the samples under studies. The shapes of the integral intensities suggest the presence of more complex magnetic entities in the compounds, at least pairs of gadolinium ions. As an example, we performed a fitting of the experimental points measured for, e.g., KYW:Gd^{3+} 10 mol% powder, applying the following Bleaney–Bowers expression for gadolinium ion electron spin $S = 7/2$:

$$I(T) = \frac{1}{T}\frac{P_1\exp(-J/kT) + P_2\exp(-3J/kT) + P_3\exp(-6J/kT) + P_4\exp(-10J/kT)}{1 + 3\exp(-J/kT) + 5\exp(-3J/kT) + 7\exp(-6J/kT) + 9\exp(-10J/kT)} + \frac{P_5\exp(-15J/kT) + P_6\exp(-21J/kT) + P_7\exp(-28J/kT)}{11\exp(-15J/kT) + 13\exp(-21J/kT) + 15\exp(-28J/kT)}, \quad (6)$$

where P_i ($i = 1, \ldots, 7$) are coefficients related to the transition probability within each multiplet of total spin $S = 0, 1, 2, 3, 4, 5, 6$ of gadolinium exchange coupled pair.[22] The intensity was directly calculated according to

the Boltzmann law,[23] yielding the total intensity from the excited energy levels of Gd^{3+} exchange coupled pair. Parameter J in the above expression is an antiferromagnetic exchange constant expressed in K. The best fit was achieved for $J = 126(8)$ K and $P_1 \cong P_2 \cong P_3 = P_4 = P_5$, $P_7 >> P_6$. It indicates strong exchange interactions between Gd^{3+} ions in the KYW:Gd^{3+} 10 mol% powder.

Figure 7 also shows that the slope of the reciprocal of integral intensities give Curie–Weiss temperatures being negative and large for the investigated compounds excluding compounds with 10 and 20 mol% concentration of Gd^{3+}. In these two cases, complex behavior can be observed. For low temperatures, up to about 140/120 K, gadolinium ions interact ferromagnetically, with Curie–Weiss temperatures equal to +14.2/33.7 K, while above the temperatures, subsequently, the interaction stays antiferromagnetic like, with Curie–Weiss temperatures equal to −16.8 and −11.3 K, respectively.

To know a reason of such behavior, we analyzed overall line widths of the registered EPR spectra. From Fig. 8, one can see that at about 140/120 K, the line widths of the EPR spectra of KYW:Gd^{3+} 10/20 mol% powders reveal maxima. The line widths of the EPR spectra of KGW and KYW:0.5 mol% of Gd^{3+} phases do not show such anomaly. So, for the two former samples, one can observe a change in magnetic ordering at least near 140/120 K, respectively.

Figure 9 presents the product of the overall magnetic intensity and a temperature, which is proportional to a square of magnetic moment of the investigated compound. Lowering of the magnetic moment with a temperature decrease is characteristic for antiferromagnetic interactions. As one can see, it is not true in a case of magnetic moment plotted for KYW:Gd^{3+} 10 and 20 mol% powders, for which, below 140/120 K, ferromagnetic behavior one can observe (growth of the magnetic moment with a decrease of temperature).

In Fig. 10, the temperature dependence of the overall resonance lines position, g, is presented. As one can see, some differences with temperature increase are observed: decrease of g for KYW:Gd^{3+} [0.5 mol% (4) and 100 mol% (3)] powders and increase for KYW:Gd^{3+} 10 mol% (1) and 20 mol% powders (2). This may be due to the presence of some internal magnetic field in the sample caused by complex interactions of gadolinium ions.

EPR spectra of KGW single crystals reveal broad asymmetric lines. The integral intensity versus temperature, equal to double integral of measured EPR signal and proportional to magnetic susceptibility, shows complex behavior of gadolinium ions. The magnetic interactions between the ions are generally antiferromagnetic like but the strength of the interactions is different below 120 K ($T_C = -3$ K) and above the temperature ($T_C = -48$ K).[8] This is the difference between Borowiec et al.[9] and our findings. The behavior is

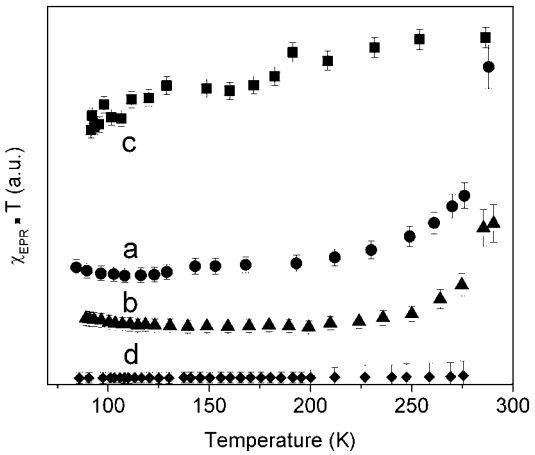

FIG. 9. Product of the overall integral intensity and a temperature for the EPR spectra of the KYW:Gd^{3+} [10 mol% (a), 20 mol% (b), 100 mol% (c), and 0.5 mol% (d)] powders.

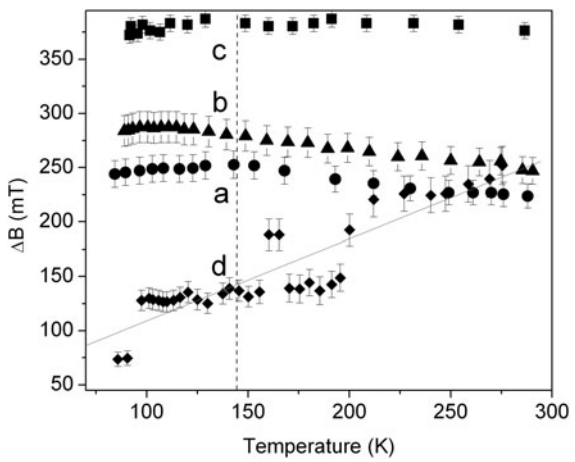

FIG. 8. Overall line widths of the KYW:Gd^{3+} [10 mol% (a), 20 mol% (b), 100 mol% (c), and 0.5 mol% (d)] powders.

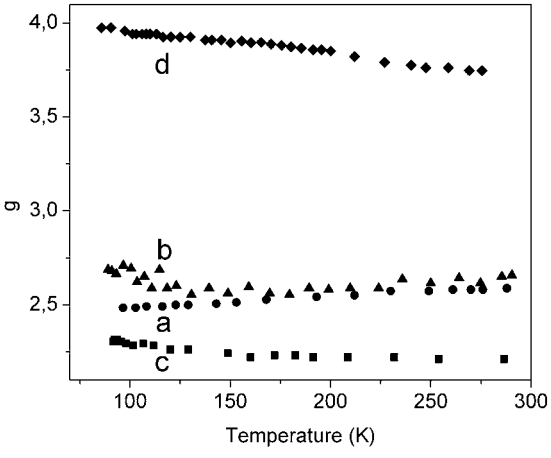

FIG. 10. The overall position of the EPR resonance lines for KYW: Gd^{3+} [10 mol% (a), 20 mol% (b), 100 mol% (c), and 0.5 mol% (d)] powders. The error bars are as high as the size of the symbols.

confirmed by the dependence of the reciprocal intensity versus temperature and the product of the integral intensity and temperature versus temperature, proportional to a square root of magnetic moment. The position of resonance line represented by g factor starts to increase from 1.67 at ~8 K to almost 1.95 when the temperature reaches ~100 K. With further increase of temperature, it becomes constant and equals to ~1.85. Such behavior of the resonance line position suggests the presence of some kind of internal magnetic fields inside KGW single crystal, assigned to, e.g., 1D, two-dimensional (2D) chains or clusters.[8] Fittings of the EPR spectra with use of the EPR-NMR program[12] expose a low local symmetry of gadolinium ions in the KGW crystal. It was found by Borowiec et al.[9] that the paramagnetic Curie temperatures in KGW crystals depend, besides a type of rare-earth ion, on magnetic field direction and have both positive and negative signs. So, their conclusions confirm our findings. The conclusions derived by Borowiec et al.[9] from magnetization measurements of KGW single crystals differ slightly from ours but they analyzed magnetization of the crystal only within the range 2–100 K. Our investigations reach room temperature range, where we found some distinct differences between KGW single crystal and KYW:Gd^{3+} powders. In the former, one can observe mainly a change in strength of antiferromagnetic-like interactions, while in the latter, besides strength, we also observed changes in magnetic ordering leading to a change in a type of magnetic interactions (in KYW powders doped with 10–20% of Gd^{3+}).

IV. CONCLUSIONS

XRD data do not show distinct differences between KGW and KYW single crystals and KYW:Gd powders in position of the diffraction peaks. Vibrational characteristics as Raman and IR spectra of samples under investigations confirm that these phases are isostructural. EPR measurements were useful to explain the changes in kind and strength of internal magnetic interactions. KGW single crystal and KGW and KYW:Gd^{3+} (0.5 mol%) powders reveal strong antiferromagnetic interactions between gadolinium ions ($T_C = -48$, -50.8, and -69.4 K, respectively). The former one shows more complex behavior below 120 K ($T_C = -3$ K) and above 120 K ($T_C = -48$ K). KYW:Gd^{3+} powders doped with 10 and 20 mol% of Gd^{3+} reveal changes in a kind of magnetic interaction at temperatures 140 and 120 K, respectively, from ferromagnetic-like behavior ($T_C = 14.2/-16.8$ K) to antiferromagnetic-like behavior (33.7/−11.3 K). This is almost the same temperature as the one recorded for the KGW single crystals (not found by Borowiec et al.[9]), now being gadolinium ion concentration dependent. The position of a resonance line, g, differs between all the compounds showing higher value for isolated gadolinium ions in KGW powders ($g > \sim 3.75$) and lower value for KGW compound ($g \sim 1.75$). In case of KGW single crystal, it is equal to ~1.85.[8] The temperature dependencies of the line position, line width, integral intensity, its reciprocal, and the product of integral intensity and temperature show on low local symmetry of gadolinium ions in all the compounds and confirm a change in a kind of magnetic interaction at 140/120 K for KGW:Gd^{3+} doped with 10 and 20 mol%, respectively. They are also evidence of a complex nature of the magnetic interactions that could be clusters or 1D, 2D chains of gadolinium ions.

ACKNOWLEDGMENTS

Authors deeply thank Dr. E. Tomaszewicz for samples synthesis and for useful comments and MSc E. Bukowska for XRD measurements.

REFERENCES

1. A.S. Kumaran, S.M. Babu, S. Ganesamoorthy, I. Bhaumik, and A.K. Karnal: Crystal growth and characterization of $KY(WO_4)_2$ and $KGd(WO_4)_2$ for laser applications. *J. Cryst. Growth* **292**, 368 (2006).
2. L. Macalik, J. Hanuza, and A.A. Kaminskii: Polarized Raman spectra of the oriented $NaY(WO_4)_2$ and $KY(WO_4)_2$ single crystals. *J. Mol. Struct.* **555**, 289 (2000).
3. P.V. Klevtsov, L.P. Kozeeva, and A.A. Pavlyuk: Polymorphism and crystallization of the potassium – rare earth molybdates KLn $(MoO_4)_2$ (Ln=La, Ce, Pr and Nd). *Kristallografiya* **20**, 1216 (1975) [in Russian].
4. C. Pujol, M. Aguiló, F. Díaz, and C. Zaldo: Growth and characterisation of monoclinic $KGd_{1-x}RE_x(WO_4)_2$ single crystals. *Opt. Mater.* **13**, 33 (1999).
5. M.C. Pujol, R. Sole, J. Massons, J. Gavalda, X. Solans, C. Zaldo, F. Diaz, and M. Aguilo: Structural study of monoclinic $KGd(WO_4)_2$ and effects of lanthanide substitution. *J. Appl. Cryst.* **34**, 1 (2001).
6. S. Perets, M. Tseitlin, R.Z. Shneck, D. Mogilyanski, G. Kimmel, and Z. Burshtein: Sodium gadolinium tungstate $NaGd(WO_4)_2$: Growth, crystallography, and some physical properties. *J. Cryst. Growth* **305**, 257 (2007).
7. L. Macalik, J. Hanuza, B. Macalik, W. Ryba-Romanowski, S. Gołąb, and A. Pietraszko: Optical spectroscopy of Dy^{3+} ions doped in $KY(WO_4)_2$ crystals. *J. Lumin.* **79**, 9 (1998).
8. H. Fuks, S.M. Kaczmarek, G. Leniec, L. Macalik, B. Macalik, and J. Hanuza: EPR and vibrational studies of some tungstates and molybdates single crystals. *Opt. Mater.* **32**, 1560 (2010).
9. M.T. Borowiec, T. Zayarnyuk, M.C. Pujol, M. Aguiló, F. Díaz, E.E. Zubov, A.D. Prokhorov, M. Berkowski, W. Domuchowski, A. Wisniewski, R. Puzniak, J. Pietosa, V.P. Dyakonov, M. Baranski, and H. Szymczak: Magnetic properties of $KRE(WO_4)_2$ (RE=Gd, Yb, Tm) single crystals. *Physica B* **405**, 4886 (2010).
10. A.S. Koster, F.X.N.M. Kools, and G.D. Rieck: The crystal structure of potassium tungstate, K_2WO_4. *Acta Crystallogr. B* **25**, 1704 (1969).
11. S.V. Borisov and R.F. Klevtsova: Crystal structure of $KY(WO_4)_2$. *Kristallografiya* **13**, 17 (1968) [in Russian].
12. M.J. Mombourquette, J.A. Weil, and D.G. McGavi: *EPR-NMR User's Manual* (Department of Chemistry, University of Saskatchewan, Saskatoon, Canada, 1999).
13. J. Viscakas, I. Mochalov, A. Mikhailov, R. Klevtsova, and A. Liubimov: Crystal structure and Raman scattering in $KGd(WO_4)_2$ crystals. *Liet. Fiz. Rinkinys* **28**, 224 (1988) [in Russian].

14. M.C. Pujol, M. Rico, C. Zaldo, R. Sole, V. Nikolov, X. Solans, M. Aguilo, and F. Diaz: Crystalline structure and optical spectroscopy of Er(3+)-doped $KGd(WO_4)_2$ single crystals. *Appl. Phys. B: Lasers Opt.* **68**, 187 (1999).
15. L. Macalik, J. Hanuza, and A.A. Kaminskii: Polarized infrared and Raman spectra of $KGd(WO_4)_2$ and their interpretation based on normal coordinate analysis. *J. Raman Spectrosc.* **33**, 92 (2002).
16. R.D. Shannon and C.T. Prewitt: Effective ionic radii in oxides and fluorides. *Acta Crystallogr. B* **25**, 925 (1969).
17. H. Fuks, S.M. Kaczmarek, L. Macalik, and J. Hanuza: EPR properties of $KY(WO_4)_2$ single crystals weakly doped with Er, Yb and Nd. *Opt. Mater.* **34**, 2086 (2012).
18. J.A. Weil and J.R. Bolton: *Electron Paramagnetic Resonance. Elementary Theory and Practical Applications*, 2nd ed. (John Wiley & Sons, Inc., Hoboken, NJ, 2007), p. 158.
19. N.V. Cherney, V.A. Nadolinny, and A.A. Pavlyuk: ESR investigation of Gd^{3+} ion introduction into the structure of simple and double tungstates. *Appl. Magn. Reson.* **33**, 45 (2008).
20. S.P. Gubin: *Magnetic Nanoparticles* (Wiley-VCH Verlag GmbH & Co. KGaA, Weinheim, 2009).
21. J. Kliava, I. Edelman, A. Potseluyko, E. Petrakovskaja, R. Berger, I. Bruckental, Y. Yeshurun, A. Malakhovskii, and T. Zarubina: EPR and magnetic properties of Gd^{3+} in oxide glasses. *J. Magn. Magn. Mater.* **272–276**, e1647 (2004).
22. N. Guskos, V. Likodimos, S. Glenis, G. Zolnierkiewicz, J. Typek, R. Szymczak, and A. Blonska-Tabero: Magnetic frustration in the site ordered $Mg_3Fe_4(VO_4)_6$ vanadate. *J. Appl. Phys.* **101**, 103922 (2007).
23. A. Bencini and D. Gatteschi: *Electron Paramagnetic Resonance of Exchange Coupled Systems* (Springer-Verlag, Berlin, 1990).